



Published in final edited form as:

J Invest Dermatol. 2013 December ; 133(12): 2722–2731. doi:10.1038/jid.2013.232.

β 1 integrins with individually disrupted cytoplasmic NPxY motifs are embryonic lethal but partially active in epidermis

Alexander Meves¹, Christopher Stremmel², Ralph Thomas Böttcher², and Reinhard Fässler²

¹Department of Dermatology, Mayo Clinic, Rochester, MN 55905; USA

²Department of Molecular Medicine, Max Planck Institute for Biochemistry, 82152 Martinsried, Germany

Abstract

β 1 integrin adhesion is believed to require binding of talins and kindlins to the membrane proximal and distal NPxY motifs of the β 1 cytoplasmic tail, respectively. To test this hypothesis we substituted the membrane proximal and distal tyrosines (Y) of the β 1 tail with alanine (A) residues (β 1 Y783A; β 1 Y795A) in the germline of mice. We report that β 1 Y783A or β 1 Y795A substitutions blocked talin or kindlin binding, respectively, and led to β 1 null-like peri-implantation lethality. Expression of β 1 Y783A or β 1 Y795A in the epidermis, however, resulted in skin blister and hair follicle phenotypes that were considerably milder than those observed with β 1 integrin gene deletion or a β 1 double Y-to-A substitution (β 1 YY783/795AA). In culture, defects in adhesion, spreading and migration were more severe with the β 1 Y783A than with the β 1 Y795A substitution despite markedly reduced β 1 Y795A integrin surface levels due to diminished protein stability. We conclude that regulation of β 1 integrin adhesion through talins and kindlins may differ substantially between stably adherent keratinocytes and cells of the developing embryo and that β 1 cytoplasmic NPxY motifs contribute individually and independent of each other to β 1 function in keratinocytes.

INTRODUCTION

Integrins are adhesion receptors that bind extracellular matrix proteins and counter receptors. When integrins bind their ligand they cluster and recruit a large number of adaptor and signaling proteins to their cytoplasmic domain to finally form cell-extracellular matrix anchoring structures called focal adhesions (FAs). FAs provide a large signaling platform, which decodes the physical and chemical qualities of the extracellular environment critically required for orchestrating tissue development and homeostasis (Legate et al., 2009; Moser et al., 2009). All integrins are composed of an α and a β subunit. The β 1 integrin subunit is ubiquitously expressed and dimerizes with 12 integrin α chains (Meves et al., 2009). Not

Corresponding author: Dr. Alexander Meves, Department of Dermatology, Mayo Clinic, 200 First St SW, Rochester, MN 55905 USA, Phone: +1 507-538-0601, Fax: +1 507-284-2072, meves.alexander@mayo.edu.

CONFLICT OF INTEREST

The authors state no conflict of interest.

surprisingly, deletion of the $\beta 1$ integrin gene in mice is embryonic lethal at peri-implantation (Fassler and Meyer, 1995).

The $\beta 1$ integrin cytoplasmic tail contains two key adaptor protein binding sites; the membrane proximal $W(x)_4NPIY$ motif that binds talins, and the membrane distal $TT(x)_2NPKY$ motif that binds kindlins (Meves et al., 2011; Moser et al., 2008). Binding of talins to the membrane proximal motif induces conformational changes in the extracellular portion of $\beta 1$ integrin that increases its affinity for extracellular matrix (Wegener et al., 2007; Ye et al., 2010). It is therefore believed that the interaction of the $\beta 1$ tail with talin precedes integrin binding to extracellular matrix in a process referred to as integrin activation or inside-out signaling. More recently, we reported that integrin activation in platelets, leukocytes and epithelial cells such as primitive endoderm and intestinal epithelial cells requires not only the binding of talins but also of kindlins to the membrane distal $NPxY$ motif (Moser et al., 2008). These findings were in contrast to reports attributing no or only a minor role to kindlins in integrin inside-out signaling (Ye et al., 2010).

To directly test the role of talin and kindlin binding to the $\beta 1$ integrin tail *in vivo*, we compared phenotypes in mice and cells carrying a Y-to-A substitution in the membrane proximal ($\beta 1$ Y783A) or distal ($\beta 1$ Y795A) $\beta 1$ $NPxY$ motif. Both mutations lead to peri-implantation lethality resembling the $\beta 1$ null phenotype. Interestingly, however, targeted expression of single Y-to-A mutations in the epidermis leads to a phenotype that is significantly milder than the $\beta 1$ -null phenotype, indicating residual activity of the $\beta 1$ Y783A and $\beta 1$ Y795A integrins. A $\beta 1$ null-like phenotype is only achieved with the simultaneous mutation of both tyrosine residues ($\beta 1$ YY783/Y795AA). These findings indicate that the functional consequences of perturbed talin and kindlin binding to $\beta 1$ integrin $NPxY$ motifs differ between cell types.

RESULTS

Single $\beta 1$ Y-to-A mutations result in peri-implantation lethality

Mice lacking $\beta 1$ integrin expression or carrying homozygous $\beta 1$ YYAA mutations die at the peri-implantation stage (Chen et al., 2006; Czuchra et al., 2006; Fassler and Meyer, 1995). To assess the *in vivo* phenotype of single $\beta 1$ cytoplasmic Y-to-A mutations and to analyze the role of talin and kindlin binding to the $\beta 1$ integrin cytoplasmic tail we generated mice with non-conservative tyrosine (Y) to alanine (A) mutations in the membrane proximal and distal $\beta 1$ integrin $NPxY$ motifs ($\beta 1$ Y783A; $\beta 1$ Y795A). The mutant knock-in (KI) alleles (KI^{neo+} ; Figure 1a) were confirmed by Southern blotting and PCR on genomic DNA derived from tail biopsies (Figure 1b, c). Deletor-Cre-mediated removal of the neomycin cassette yielded mice with heterozygous $\beta 1$ Y783A or Y795A mutations, respectively. They were healthy and fertile. Progeny of heterozygous crossings yielded wild-type and heterozygous but no homozygous offspring (Figure 1d).

To assess the embryonic defects of mice with single $\beta 1$ cytoplasmic Y-to-A mutations, we performed timed heterozygous matings and analyzed the gross morphology of embryos at embryonic day (E) 7.5. Compared to wild-type embryos, $\beta 1$ Y783A and Y795A embryos were severely malformed indicating that the embryos die at the peri-implantation stage

(Figure 1e). To better define the cause of death during early development, we established ES cell cultures from homozygous $\beta 1$ Y783A and Y795A blastocysts. Similar to $\beta 1$ -null and $\beta 1$ YY783/795AA (YYAA) ES cells, single $\beta 1$ Y-to-A ES cells adhered less to feeder cells (Figure 1f). We then generated embryoid bodies (EBs) from wild-type or mutant ES cells to further study peri-implantation development (Montanez et al., 2007). The formation of wild-type EBs from an aggregate of ES cells followed a series of events starting with the formation of an outer layer of endoderm cells which secret and assemble a laminin-rich basement membrane, followed by the conversion of the undifferentiated core into a layer of pseudo-stratified primitive ectoderm and a central cavity on day 4 to 6 (Figure 1g) (Böttcher et al., 2012). In contrast, single $\beta 1$ Y-to-A and $\beta 1$ YYAA EBs formed compact aggregates with significant detachment of the endoderm cell layer, abnormally assembled and often discontinuous basement membrane and absent cavity formation, which resembled the defects of $\beta 1$ -null EBs (Figure 1g, h) (Li et al., 2002).

Fluorescence-activated cell sorting (FACS) analysis revealed an apparently normal expression of $\beta 1$ integrin on ES cells carrying the membrane proximal $\beta 1$ Y783A mutation (Figure 1i). As expected, $\beta 1$ integrin surface levels on ES cells carrying the membrane distal Y795A mutation were significantly reduced (Figure 1i) due to the impaired recruitment of SNX17 to the $\beta 1$ Y795A tails in early and recycling endosomes, which prevents lysosomal $\beta 1$ degradation (Böttcher et al., 2012). The $\beta 1$ heterodimerization partners $\alpha 5$ and $\alpha 6$ integrin were also reduced in $\beta 1$ Y795A ES cells, while $\alpha v\beta 3$ integrin surface levels were normal (Figure 1i). As expected, all $\beta 1$ Y-to-A mutated integrins had reduced extracellular ligand binding activity as assessed by the reduced availability of 9EG7 epitope during FACS (Figure 1j) and reduced adhesion to fibronectin and laminin (LN) 111 (Figure 1k).

Compound heterozygous $\beta 1^{Y783A/Y795A}$ mice die at peri-implantation

The availability of the $\beta 1$ Y783A and Y795A mouse strains allowed the generation of compound heterozygous ($\beta 1^{Y783A/Y795A}$) animals that enable kindlin binding to the $\beta 1$ Y783A and talin binding to the $\beta 1$ Y795A allele and thus, testing whether talin and kindlin cooperate with each other in a *trans* configuration (Moser et al., 2009). Intercrosses of the $\beta 1$ Y783A strain with the Y795A strain revealed no live offspring. The dissection of decidua chambers at different stages of pregnancy showed that the $\beta 1^{Y783A/Y795A}$ compound mice died at the peri-implantation stage with a phenotype that resembled the homozygous $\beta 1$ Y783A or $\beta 1$ Y795A mutations (Figure 2a). $\beta 1^{Y783A/Y795A}$ ES cells were less adhesive compare to wild-type (Figure 2b) and EBs derived from $\beta 1^{Y783A/Y795A}$ ES cells showed defects similar to $\beta 1$ -null EBs (Figure 2c,d). $\beta 1$ integrin surface levels (Figure 2e), 9EG7 epitope availability (Figure 2f) and cell adhesion to fibronectin and LN111 (Figure 2g) were reduced to a similar extent as observed with the homozygous $\beta 1$ Y795A mutation.

Single $\beta 1$ Y-to-A integrin is partially active in keratinocytes

To test whether the $\beta 1$ Y-to-A mutations also lead to $\beta 1$ -null-like phenotypes in other cell types we decided to express the $\beta 1$ Y783A or $\beta 1$ Y795A mutations in the epidermal keratinocytes. Epidermal keratinocytes were chosen because they lack $\beta 3$ integrin, express low levels of αv integrin and predominantly express $\beta 1$ integrin. To achieve hemizygous targeted expression of the knock-in alleles in epidermis, we intercrossed a floxed (fl) $\beta 1$

allele with the $\beta 1$ Y-to-A alleles or with a non-floxed wild-type $\beta 1$ gene (control) and ablated the floxed $\beta 1$ gene using a keratin (K) 5 promoter-driven Cre recombinase (Figure 3a). Since the floxed $\beta 1$ integrin allele was designed to couple genomic $\beta 1$ integrin deletion to the activation of a lacZ gene (Brakebusch et al., 2000), successful Cre activity can be readily detected in the epidermis and hair follicles of hemizygous wild-type and $\beta 1$ Y-to-A skin by immunohistochemistry (Figure 3b) and flow cytometry (Figure 3c). Deletion of homozygous $\beta 1^{fl/fl}$ integrin alleles by K5-Cre (Brakebusch et al., 2000) or hemizygous expression of $\beta 1$ YYAA in epidermis (Czuchra et al., 2006) leads to a near complete loss of terminal hair in mice and reduced weight gain. In contrast to this marked phenotype, $\beta 1$ Y783A or $\beta 1$ Y795A epidermis showed patchy hair loss over the dorsal midline of the skull in $\beta 1$ Y783A epidermis (Figure 3d) but otherwise no additional defects on gross inspection. This finding suggests that the activities of the mutant integrins are not or only marginally affected by impaired talin or kindlin binding.

To further test whether the $\beta 1$ Y783A or the $\beta 1$ Y795A integrins are indeed partially active in epidermis, we analyzed skin histologically (Figure 3d). $\beta 1$ -null epidermis is characterized by subepidermal blistering, patchy deposition of laminin 332 in the papillary dermis, impaired hemidesmosome assembly and dermal inflammatory infiltrates that induce hyperproliferation of basal keratinocytes (Brakebusch et al., 2000). The same phenotype was also seen in $\beta 1$ YYAA epidermis (Figure 3d) (Czuchra et al., 2006). In contrast, single $\beta 1$ Y-to-A epidermis was less affected. We observed linear deposition of $\alpha 6$ integrin at the dermato-epidermal junction, demonstrating proper localization of hemidesmosomes, and normal proliferation in the skin as indicated by the single layer of K5 expressing basal keratinocytes and normal numbers of Ki67-positive cells (wild-type: 6 ± 3 ; $\beta 1$ Y783A: 8 ± 3 ; $\beta 1$ Y795A: 8 ± 3 ; $\beta 1$ YYAA: 18 ± 1 Ki67 positive cells per high-powered field) Laminin 332 deposition was focally shaggy and abnormal, however, not to the extent observed with $\beta 1$ YYAA epidermis. Interestingly, we failed to observe subepidermal blistering indicating the ability of basal keratinocytes to firmly adhere to the underlying basement membrane. As expected from the focal hair loss *in vivo*, we saw impaired hair follicle morphogenesis in $\beta 1$ Y783A but not $\beta 1$ Y795A skin; enlarged hair follicle stumps were seen intermixed with normally shaped thin hair follicles extending deep into the subcutaneous fat. In $\beta 1$ YYAA as well as $\beta 1$ -null epidermis, all hair follicles were enlarged and abnormal. In summary these findings suggest that keratinocytes expressing either the $\beta 1$ Y783A or the $\beta 1$ Y795A substitution must possess residual $\beta 1$ activity.

Distinct consequences of $\beta 1$ Y783A and $\beta 1$ Y795A mutations on $\beta 1$ function in keratinocytes

The subtle defects of $\beta 1$ Y783A or the $\beta 1$ Y795A epidermis *in vivo* prompted us to analyze $\beta 1$ integrin functions *ex vivo*. In line with the findings from the mutant ES cells, flow cytometry revealed normal expression levels of $\beta 1$ Y783A and markedly reduced levels of $\beta 1$ Y795A and $\beta 1$ YYAA on freshly isolated primary keratinocytes (Figure 4a). Despite the normal $\beta 1$ Y783A levels keratinocytes exhibited defects in adhesion (Figure 4b) and spreading that were more pronounced compared with $\beta 1$ Y795A keratinocytes (Figure 4c). $\beta 1$ YYAA keratinocytes did not adhere (Figure 4b) (Czuchra et al., 2006). $\beta 1$ Y783A keratinocytes did not grow into confluent monolayers but instead become large and flat and

rapidly initiated terminal differentiation (Figure 4b). In contrast, $\beta 1$ Y795A keratinocytes underwent normal spreading, proliferated and consistently formed confluent monolayer in culture. Scratch wounding assays demonstrated that $\beta 1$ Y795A keratinocytes were able to close the *in vitro* wound, although slower than wild-type (Figure 4d and e). Single-cell tracking revealed that $\beta 1$ Y795A keratinocytes migrated directionally (Figure 4f) but with reduced speed when compared to wild-type (Figure 4g). Since $\beta 1$ Y783A keratinocytes were unable to form monolayers *in vitro* we were unable to perform scratch assays.

In summary, the $\beta 1$ Y783A mutation allows normal surface expression but impairs keratinocyte adhesion, spreading and proliferation. The $\beta 1$ Y795A mutation reduces $\beta 1$ integrin surface expression and migration speed but allows normal adhesion, spreading and proliferation of keratinocyte. The $\beta 1$ YYAA mutation abrogates all $\beta 1$ integrin functions.

Distinct consequences of $\beta 1$ Y783A and $\beta 1$ Y795A mutations on $\beta 1$ function in fibroblasts

$\beta 1$ Y783A and $\beta 1$ YYAA keratinocytes poorly adhered and did not grow in culture due to terminal differentiation. To further characterize the cellular phenotype of single and double $\beta 1$ Y-to-A mutations, we decided to reconstitute $\beta 1$ -null fibroblasts with wild-type, $\beta 1$ Y783A, $\beta 1$ Y795A or $\beta 1$ YYAA integrins by retroviral cDNA transduction (Figure 5a) (Böttcher et al., 2012). In contrast to keratinocytes, fibroblasts express $\beta 3$ integrin, which partially compensates for the loss in $\beta 1$ integrin-mediated adhesion. FACS analysis showed reduced $\beta 1$ integrin surface levels in $\beta 1$ Y795A cells while the levels of other $\beta 1$ Y-to-A variants were comparable to wild-type $\beta 1$ integrin surface levels (Figure 5b). Similar to primary keratinocytes, $\beta 1$ Y795A and wild-type fibroblasts were well-spread whereas $\beta 1$ Y783A and $\beta 1$ YYAA fibroblasts resembled the more rounded $\beta 1$ -null cells (Figure 5c). Interestingly, Y-to-A mutation in the Y783A motif significantly impaired internalization of cell surface $\beta 1$ integrin (Figure 5d), while $\beta 1$ integrin stability was only reduced after Y-to-A mutation of the Y795A motif (Figure 5e). In single-cell migration assays on fibronectin all $\beta 1$ Y-to-A mutations exhibited reduced cell velocity (Figure 5f and g). However, the velocity defect was least pronounced with the membrane distal $\beta 1$ Y795A mutation.

In summary, the phenotypes of the $\beta 1$ Y-to-A mutations were similar in fibroblast and keratinocytes. Specifically, $\beta 1$ Y783A mutations had a greater impact on spreading and migration than $\beta 1$ Y795A mutations. The latter however significantly impaired integrin half-life.

Talin and kindlin recruitment is affected by the $\beta 1$ cytoplasmic Y-to-A mutations

The subtle defects of the of the $\beta 1$ Y783A or the $\beta 1$ Y795A epidermis *in vivo* suggest a less prominent role for talin and kindlin binding to the $\beta 1$ tails than in ES cells (Montanez et al., 2008). Therefore, we tested to which degree $\beta 1$ NPxY motifs were disrupted by single ($\beta 1$ Y783A, $\beta 1$ Y795A) or double ($\beta 1$ YYAA) $\beta 1$ Y-to-A mutations in keratinocytes versus ES cells by performing pulldown experiments with synthesized peptides corresponding to wild-type and $\beta 1$ Y-to-A mutated $\beta 1$ integrin cytoplasmic tails using SILAC-labeled ES cell and keratinocyte protein lysates followed by quantification of precipitated proteins using mass spectrometry (Meves et al., 2011) (Figure 6a). We found that the $\beta 1$ YYAA peptide completely lost the ability to recruit proteins from both keratinocyte and ES cell lysates

when compared to a scrambled peptide sequence (Figure 6b–e). Specifically, binding of talins and kindlins was completely abolished in keratinocytes (Figure 6c) and ES cells (Figure 6e). Selective disruption of single NPxY motifs by $\beta 1$ Y-to-A substitutions only prevented binding of a specific subset of proteins, most notably talins or kindlins to the membrane proximal or distal NPxY motifs, respectively (Figure 6f and g). This observation was made with keratinocyte (Mathew et al., 2012) and ES cell lysates.

DISCUSSION

Single disrupted $\beta 1$ cytoplasmic NPxY motifs have been predicted to prevent talin and kindlin binding to $\beta 1$ tails and therefore, to result in $\beta 1$ integrin loss-of-function (Moser et al., 2009). Consistent with established models of integrin activation (Ye et al., 2012), we found that both single $\beta 1$ Y-to-A mutations were early embryonic lethal and resulted in $\beta 1$ -null-like *in vivo* phenotypes and *ex vivo* EB defects. The same observations were made for compound heterozygous $\beta 1^{Y783A/Y795A}$ mice, supporting a role for both adaptor proteins on the same $\beta 1$ integrin tail and thus, lack of $\beta 1$ integrin *trans* activation through talins and kindlins (Moser et al., 2009). Unexpectedly, the epidermis exhibited a $\beta 1$ -null phenotype only when both $\beta 1$ NPxY motifs were disrupted, while single Y-to-A mutations resulted in subtle defects. Mice harboring single $\beta 1$ Y-to-A mutations in either the talin or kindlin binding sites retained a fully attached and normally differentiated epidermis with minor abnormalities in basement membrane structure, indicating only minor impairment of $\beta 1$ integrin function.

Talin binding has long been viewed as the ‘on-switch’ for integrins by inducing a high affinity state for extracellular ligand (Tadokoro et al., 2003; Ye et al., 2010). Absence of this interaction was thought to yield integrins unable to adhere and signal. Our study, however, shows that models of $\beta 1$ integrin regulation that predict activity based on talin recruitment are oversimplified. It becomes increasingly clear that the regulation of integrin activity is multi-faceted. In addition to talins, kindlins are required for affinity regulation in cells that need rapid integrin adhesion (Montanez et al., 2008; Moser et al., 2008; Ussar et al., 2008). Other mechanisms such as mechanical force (Friedland et al., 2009; Schiller et al., 2011; Shi and Boettiger, 2003), clustering (Roca-Cusachs et al., 2009), chemical modifications (Isaji et al., 2010), compartmentalization (Larkin et al., 2009), trafficking (Margadant et al., 2011) and stability (Böttcher et al., 2012) exert important additional spatiotemporal control of integrin functions. It appears likely that the latter become particularly important to cells that do not require rapid regulation of adhesion. In contrast to platelets or leukocytes, basal keratinocytes are stably exposed to ligand of the basement membrane, and integrin-extracellular matrix bonds may form and dissolve continuously without affinity modulation by adaptor proteins (Boettiger, 2012). Stable adhesions may form primarily as a consequence of adhesion strengthening, a process that involves mechanical force (Schiller et al., 2011) or clustering of integrins (Paszek et al., 2009). These processes also require adaptor protein binding to $\beta 1$ integrin NPxY motifs (Feng et al., 2012; Zhang et al., 2008). However, in contrast to affinity modulation, disruption of either $\beta 1$ NPxY is insufficient to block their roles completely.

While effective affinity modulation requires binding of talins *and* kindlins, e.g. in platelets (Moser et al., 2008) or ES cells (Montanez et al., 2008), stabilization of the $\beta 1$ integrin-ligand interaction in cells that are continuously adhere to the extracellular matrix such as keratinocytes occurs, at least to a certain extent, even in the absence of direct talin or kindlin binding to the $\beta 1$ integrin cytoplasmic domain. While both $\beta 1$ NPxY motives have unique properties such as the regulation of $\beta 1$ protein stability via the distal NPxY, each $\beta 1$ NPxY motif couples to the actin cytoskeleton through its respective focal adhesion-based adaptor protein talin or kindlin, and thus may be used independently to strengthen the integrin-ligand interaction through catch bonds, i.e. integrin-ligand bonds that increase in stability and lifetime through acto-myosin-mediated pulling (Boettiger, 2012). Hence, deletion of a single NPxY motif would not eliminate but only reduce the ability of a cell to regulate integrin adhesion through force. In contrast, deletion of both NPxY motifs would eliminate all $\beta 1$ integrin adhesion, as was found in this study.

In summary, $\beta 1$ integrin adhesion in the absence of either talin or kindlin binding is possible but significantly delayed and functionally compromised. While epidermis is well equipped to compensate for some of the consequences of deficient $\beta 1$ integrin function, e.g. through the hemidesmosomal $\alpha 6\beta 4$ integrin, other types of adhesion receptors such as dystroglycans, or other yet unknown cell-type specific adaptor proteins, this may not be the case for the developing embryo, which depends on the mechanical and signaling support of $\beta 1$ integrin. In addition, the developing embryo is a rapidly evolving organism that likely needs to regulate adhesion quickly and may therefore depend on $\beta 1$ integrin affinity regulation.

MATERIALS AND METHODS

Generation of mice

Mice with $\beta 1$ YYAA and $\beta 1$ Y795A mutations were reported previously (Böttcher et al., 2012; Czuchra et al., 2006). Mouse genomic DNA used to generate the targeting vector for the $\beta 1$ Y783A knock-in and the targeting strategy were as previously described (Czuchra et al., 2006; Fassler and Meyer, 1995). Upon germline transmission, mutant mice were intercrossed with deleter-Cre transgenic mice (Czuchra et al., 2006) to remove the neomycin cassette. Compound heterozygous $\beta 1^{Y783A/Y795A}$ ES cells and embryos were generated by inter-crossing heterozygous $\beta 1$ Y783A with $\beta 1$ Y795A animals. All animal studies were approved by the Regierung von Oberbayern.

Flow cytometry

Flow cytometry of freshly isolated keratinocytes and ES cells was as previously described (Böttcher et al., 2012; Czuchra et al., 2006). The following antibodies were used: $\beta 1$ integrin PE (102207, HMB1-1, BioLegend; 1:400), $\beta 1$ integrin 9EG7 (550531, 9EG7, BD Pharmingen; 1:100), $\beta 3$ integrin PE (12-0611, 2C9.G3, eBioscience; 1:400), $\alpha 5$ -integrin PE (557447, 5H10-27, BD Pharmingen; 1:400), $\alpha 6$ -integrin PE (555736, GoH3, BD Pharmingen) and αv -integrin PE (551187, RMV-7, BD; 1:400). Dilutions were as previously described (Czuchra et al., 2006).

Immunohistochemistry

The following antibodies were used for immunohistochemistry: β 1 integrin (MAB1997, Millipore), laminin 111 (ab30320, Abcam), laminin 332 (a kind gift from M. Aumailley, University of Cologne, Cologne, Germany), α 6 integrin-FITC (BD Biosciences) and keratin 5 (ab24647, Abcam). β -Galactosidase activity was determined as previously described (Czuchra et al., 2006).

SILAC-based peptide pulldowns

Pulldowns were performed as previously described (Meves et al., 2011).

ES cells and embryoid bodies

ES cells were isolated and cultured as previously described (Böttcher et al., 2012). Embryoid bodies were generated as described previously (Böttcher et al., 2012).

Isolation of primary keratinocytes, adhesion, spreading, and migration assays

Primary keratinocytes were isolated from P21 mice and grown to confluence as previously described (Czuchra et al., 2006; Meves et al., 2011). Adhesion of ES cells and primary keratinocytes to fibronectin, laminin and collagen I and cell spreading were performed and analyzed as described previously (Böttcher et al., 2012; Czuchra et al., 2006). Cell wounding was performed as previously described (Lorenz et al., 2007). Live-cell recordings were performed immediately after wounding for 12 h at 37°C and 5% CO₂. At least four independent scratch-wound experiments were used for calculations. Single-cell tracking of cells within the leading edge was performed using MetaMorph software, choosing 15 cells each in at least three independent experiments.

β 1 Y-to-A fibroblast lines

Point mutations of β 1 integrin cDNA (β 1 Y783A, β 1 Y795A, β 1 YY783/795AA) were introduced by site-directed mutagenesis. For stable expression in fibroblasts, β 1 integrin cDNA was cloned into the retroviral expression vectors pCLMFG or pLZRS. Viral particles were concentrated from cell culture supernatant as described previously (Pfeifer et al., 2000) and used for infection.

Integrin stability and internalization

This was determined as previously described (Böttcher et al., 2012).

ACKNOWLEDGMENTS

This work was funded by the Max Planck Society, the DFG (SFB 914) and the Mayo Clinic.

REFERENCES

- Boettiger D. Mechanical control of integrin-mediated adhesion and signaling. *Curr Opin Cell Biol.* 2012; 24:592–599. [PubMed: 22857903]
- Böttcher RT, Stremmel C, Meves A, Meyer H, Widmaier M, Tseng HY, Fässler R. Sorting nexin 17 prevents lysosomal degradation of [beta] 1 integrins by binding to the [beta] 1-integrin tail. *Nat Cell Biol.* 2012; 14:584–592. [PubMed: 22561348]

- Brakebusch C, Grose R, Quondamatteo F, Ramirez A, Jorcano JL, Pirro A, Svensson M, Herken R, Sasaki T, Timpl R, et al. Skin and hair follicle integrity is crucially dependent on beta 1 integrin expression on keratinocytes. *EMBO J.* 2000; 19:3990–4003. [PubMed: 10921880]
- Chen H, Zou Z, Sarratt KL, Zhou D, Zhang M, Sebzda E, Hammer DA, Kahn ML. In vivo beta1 integrin function requires phosphorylation-independent regulation by cytoplasmic tyrosines. *Genes Dev.* 2006; 20:927–932. [PubMed: 16618804]
- Cox J, Mann M. MaxQuant enables high peptide identification rates, individualized p.p.b.-range mass accuracies and proteome-wide protein quantification. *Nat Biotechnol.* 2008; 26:1367–1372. [PubMed: 19029910]
- Czuchra A, Meyer H, Legate KR, Brakebusch C, Fassler R. Genetic analysis of beta1 integrin "activation motifs" in mice. *J Cell Biol.* 2006; 174:889–899. [PubMed: 16954348]
- Fassler R, Meyer M. Consequences of lack of beta 1 integrin gene expression in mice. *Genes Dev.* 1995; 9:1896–1908. [PubMed: 7544313]
- Feng C, Li YF, Yau YH, Lee HS, Tang XY, Xue ZH, Zhou YC, Lim WM, Cornvik TC, Ruedl C. Kindlin-3 Mediates Integrin α L β 2 Outside-in Signaling, and It Interacts with Scaffold Protein Receptor for Activated-C Kinase 1 (RACK1). *J Biol Chem.* 2012; 287:10714. [PubMed: 22334666]
- Friedland JC, Lee MH, Boettiger D. Mechanically activated integrin switch controls alpha5beta1 function. *Science.* 2009; 323:642–644. [PubMed: 19179533]
- Isaji T, Kariya Y, Xu Q, Fukuda T, Taniguchi N, Gu J. Functional roles of the bisecting GlcNAc in integrin-mediated cell adhesion. *Methods Enzymol.* 2010; 480:445–459. [PubMed: 20816221]
- Larkin D, Treumann A, Murphy D, DeChaumont C, Kiernan A, Moran N. Compartmentalization regulates the interaction between the platelet integrin α IIB β 3 and ICln. *Br J Haematol.* 2009; 144:580–590. [PubMed: 19055659]
- Legate KR, Wickström SA, Fässler R. Genetic and cell biological analysis of integrin outside-in signaling. *Genes Dev.* 2009; 23:397–418. [PubMed: 19240129]
- Li S, Harrison D, Carbonetto S, Fässler R, Smyth N, Edgar D, Yurchenco PD. Matrix assembly, regulation, and survival functions of laminin and its receptors in embryonic stem cell differentiation. *J Cell Biol.* 2002; 157:1279–1290. [PubMed: 12082085]
- Lorenz K, Grashoff C, Torka R, Sakai T, Langbein L, Bloch W, Aumailley M, Fassler R. Integrin-linked kinase is required for epidermal and hair follicle morphogenesis. *J Cell Biol.* 2007; 177:501–513. [PubMed: 17485490]
- Margadant C, Monsuur HN, Norman JC, Sonnenberg A. Mechanisms of integrin activation and trafficking. *Curr Opin Cell Biol.* 2011; 23:607–614. [PubMed: 21924601]
- Mathew S, Lu Z, Palamuttam RJ, Mernaugh G, Hadziselimovic A, Chen J, Bulus N, Gewin LS, Voehler M, Meves A, et al. β 1 Integrin NPXY Motifs Regulate Kidney Collecting-Duct Development and Maintenance by Induced-Fit Interactions with Cytosolic Proteins. *Mol Cell Biol.* 2012; 32:4080–4091. [PubMed: 22869523]
- Meves A, Geiger T, Zanivan S, DiGiovanni J, Mann M, Fassler R. [beta]1 integrin cytoplasmic tyrosines promote skin tumorigenesis independent of their phosphorylation. *Proc Natl Acad Sci U S A.* 2011; 108:15213–15218. [PubMed: 21876123]
- Meves A, Stremmel C, Gottschalk K, Fassler R. The Kindlin protein family: new members to the club of focal adhesion proteins. *Trends Cell Biol.* 2009; 19:504–513. [PubMed: 19766491]
- Montanez E, Piwko-Czuchra A, Bauer M, Li S, Yurchenco P, Fässler R. Analysis of Integrin Functions in Peri-Implantation Embryos, Hematopoietic System, and Skin. *Methods Enzymol.* 2007; 426:239–289. [PubMed: 17697888]
- Montanez E, Ussar S, Schifferer M, Bosl M, Zent R, Moser M, Fassler R. Kindlin-2 controls bidirectional signaling of integrins. *Genes Dev.* 2008; 22:1325–1330. [PubMed: 18483218]
- Moser M, Legate KR, Zent R, Fassler R. The tail of integrins, talin, and kindlins. *Science.* 2009; 324:895–899. [PubMed: 19443776]
- Moser M, Nieswandt B, Ussar S, Pozgajova M, Fässler R. Kindlin-3 is essential for integrin activation and platelet aggregation. *Nat Med.* 2008; 14:325–330. [PubMed: 18278053]
- Paszek MJ, Boettiger D, Weaver VM, Hammer DA. Integrin clustering is driven by mechanical resistance from the glycocalyx and the substrate. *PLoS Comput Biol.* 2009; 5:e1000604. [PubMed: 20011123]

- Pfeifer A, Kessler T, Silletti S, Cheresh DA, Verma IM. Suppression of angiogenesis by lentiviral delivery of PEX, a noncatalytic fragment of matrix metalloproteinase 2. *Proc Natl Acad of Sci U S A*. 2000; 97:12227–12232. [PubMed: 11035804]
- Roberts M, Barry S, Woods A, van der Sluijs P, Norman J. PDGF-regulated rab4-dependent recycling of $\alpha v\beta 3$ integrin from early endosomes is necessary for cell adhesion and spreading. *Curr Biol*. 2001; 11:1392–1402. [PubMed: 11566097]
- Roca-Cusachs P, Gauthier NC, Del Rio A, Sheetz MP. Clustering of $\alpha 5\beta 1$ integrins determines adhesion strength whereas $\alpha v\beta 3$ and talin enable mechanotransduction. *Proc Natl Acad of Sci U S A*. 2009; 106:16245–16250. [PubMed: 19805288]
- Schiller HB, Friedel CC, Boulegue C, Fassler R. Quantitative proteomics of the integrin adhesome show a myosin II-dependent recruitment of LIM domain proteins. *EMBO Rep*. 2011; 12:259–266. [PubMed: 21311561]
- Shi Q, Boettiger D. A novel mode for integrin-mediated signaling: tethering is required for phosphorylation of FAK Y397. *Mol Biol Cell*. 2003; 14:4306–4315. [PubMed: 12960434]
- Tadokoro S, Shattil SJ, Eto K, Tai V, Liddington RC, de Pereda JM, Ginsberg MH, Calderwood DA. Talin binding to integrin beta tails: a final common step in integrin activation. *Science*. 2003; 302:103–106. [PubMed: 14526080]
- Ussar S, Moser M, Widmaier M, Rognoni E, Harrer C, Genzel-Boroviczeny O, Fassler R. Loss of Kindlin-1 causes skin atrophy and lethal neonatal intestinal epithelial dysfunction. *PLoS Genet*. 2008; 4:e1000289. [PubMed: 19057668]
- Wegener KL, Partridge AW, Han J, Pickford AR, Liddington RC, Ginsberg MH, Campbell ID. Structural basis of integrin activation by talin. *Cell*. 2007; 128:171–182. [PubMed: 17218263]
- Ye F, Hu G, Taylor D, Ratnikov B, Bobkov AA, McLean MA, Sligar SG, Taylor KA, Ginsberg MH. Recreation of the terminal events in physiological integrin activation. *J Cell Biol*. 2010; 188:157–173. [PubMed: 20048261]
- Ye F, Kim C, Ginsberg MH. Reconstruction of integrin activation. *Blood*. 2012; 119:26–33. [PubMed: 21921044]
- Zhang X, Jiang G, Cai Y, Monkley SJ, Critchley DR, Sheetz MP. Talin depletion reveals independence of initial cell spreading from integrin activation and traction. *Nat Cell Biol*. 2008; 10:1062–1068. [PubMed: 19160486]

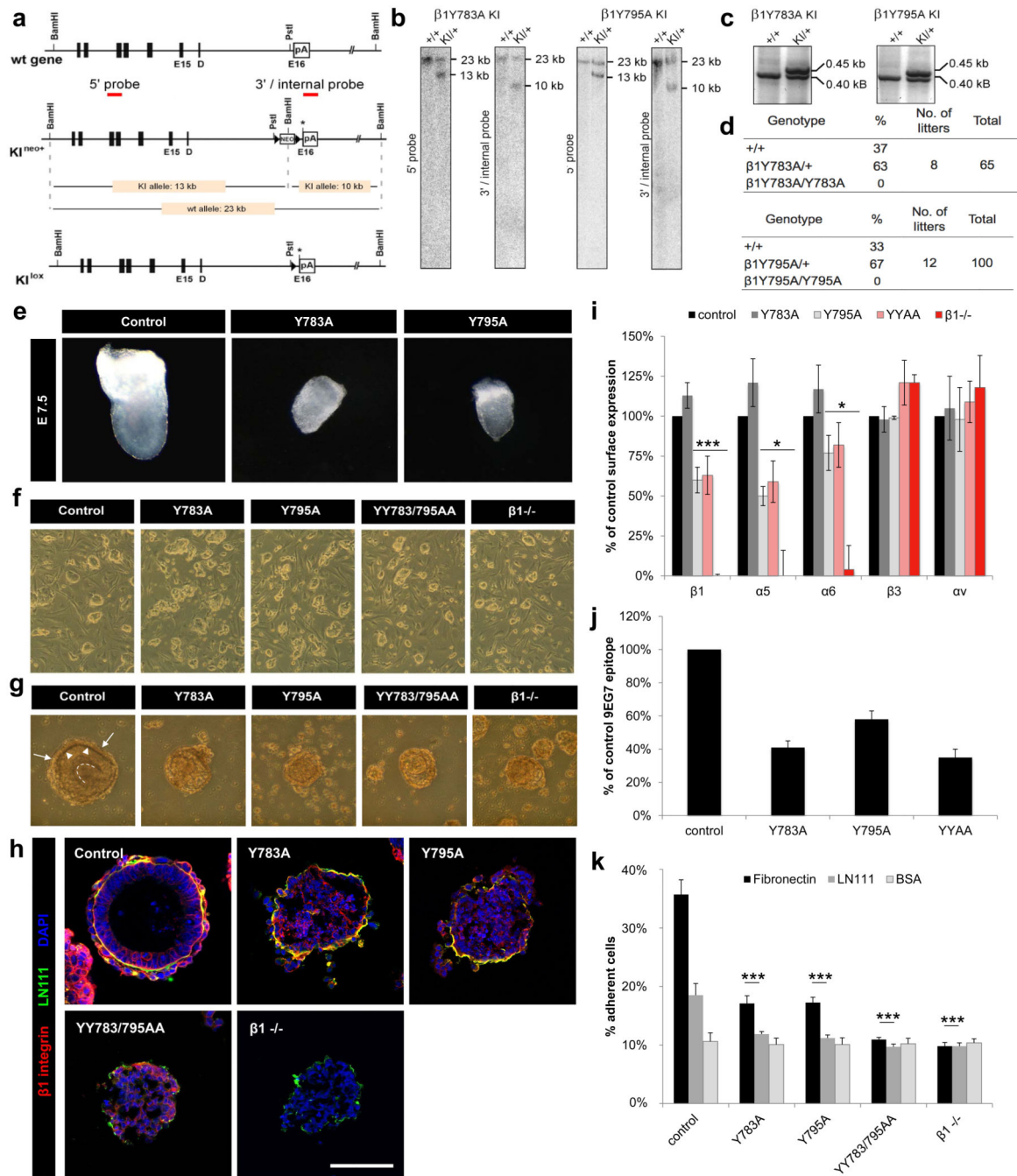


Figure 1. β1 Y-to-A mutations cause a β1-null-like phenotype in ES cells

(a) Partial map of β1 wild-type (wt) and knock-in (KI) alleles before (KI^{neo+}) and after (KI^{lox}) neo deletion through Cre. Asterisk: site of point mutagenesis. Triangles: loxP sites. (b) Southern blotting identified homologous recombination. (c) PCR genotyping of KI^{lox} mice using loxP site flanking primers. (d) Numbers and genotypes of offspring from heterozygous crossings. (e) Bright field images of E7.5 embryos. (f) ES cell colonies on feeder cells. (g–h) Bright field and immunofluorescence images of EBs on day 5 of suspension culture. (g) Arrows: endoderm cells. Arrowheads: BM. Dotted line: central

cavity lining. **(h)** EBs were stained with antibodies against $\beta 1$ integrin (red) and Laminin 111 (green) and nuclei were counterstained with DAPI (blue). Scale bar=100 μ m. **(i)** Expression of integrin subunits on ES cells by FACS (mean \pm SD; n=4; * P <0.05, *** P <0.0001 vs. control). **(j)** Quantification of the 9EG7 epitope by FACS (mean \pm SD; n=4). **(k)** Quantification of cell adhesion (mean \pm SD; n=4; *** P <0.0001 vs. control). LN111, Laminin 111; BSA, bovine serum albumin.

Author Manuscript

Author Manuscript

Author Manuscript

Author Manuscript

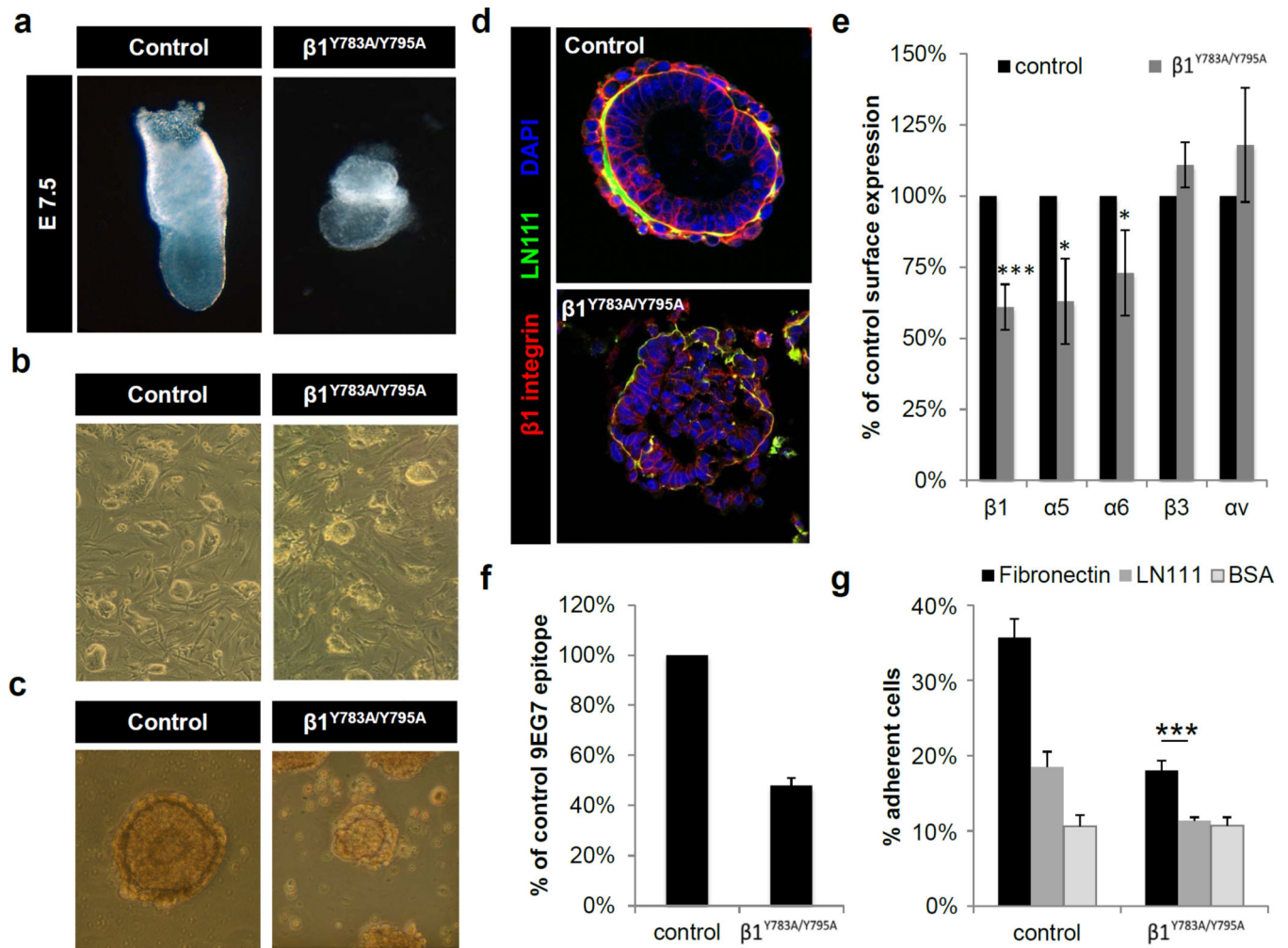


Figure 2. Absence of $\beta 1$ integrin *trans* activation in compound heterozygous $\beta 1^{Y783A/Y795A}$ embryos

(a) Bright field images of E7.5 embryos. (b) ES cell colonies on feeder cells. (c–d) Bright field (c) and immunofluorescence images (d) of embryoid bodies on the 5th day of suspension culture. EBs were stained with antibodies against $\beta 1$ integrin (red) and Laminin 111 (green) and nuclei were counterstained with DAPI (blue). Scale bar=100 μ m. (e) Expression of integrin subunits on ES cells determined by FACS (mean \pm SD; n=4; * P <0.05, *** P <0.0001 vs. control). (f) Integrin activation on ES cells measured by 9EG7 binding (mean \pm SD; n=4). (g) Quantification of cell adhesion (*** P <0.0001 vs. control). LN111, Laminin 111; BSA, bovine serum albumin.

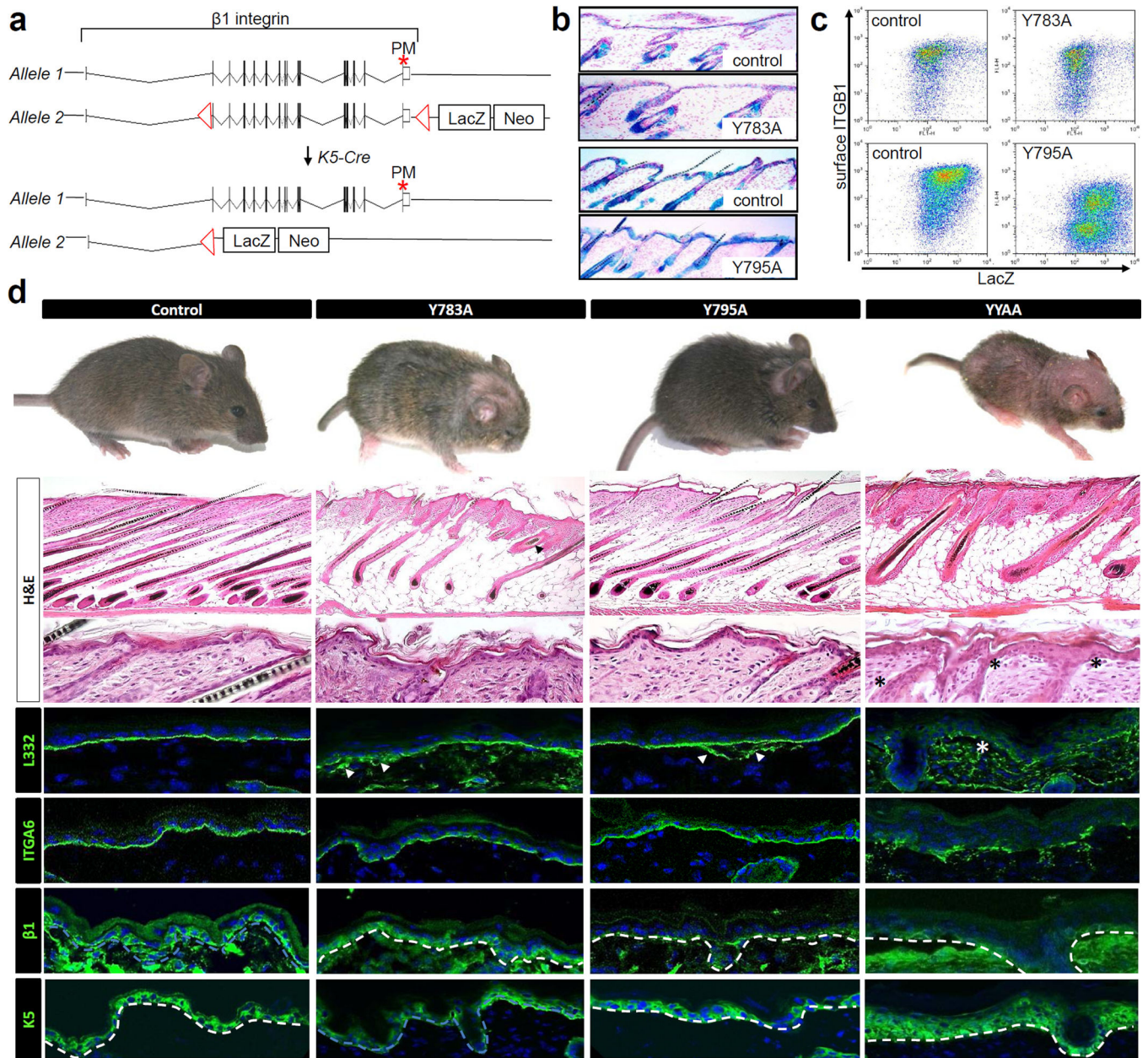


Figure 3. Single $\beta 1$ Y-to-A integrin is partially active in keratinocytes

(a) Approach for achieving hemizygous $\beta 1$ Y-to-A integrin expression in epidermis. Exon structure of $\beta 1$ integrin is depicted. Site of point mutation is highlighted by an asterisk. LoxP sites are shown as triangles. Recombination of $\beta 1^{fl/fl}$ loxP sites by Cre results in LacZ transcription (b and c) Detection of LacZ activity by immunohistochemistry (b) or flow cytometry (c). (d) Gross morphology and histological analysis of mice and epidermis with single or double $\beta 1$ Y-to-A mutations at postnatal day 14. Dotted lines: dermoepidermal junction. Asterisks: subepidermal split. White arrow heads: non-linear sub-epidermal LN332 deposition.

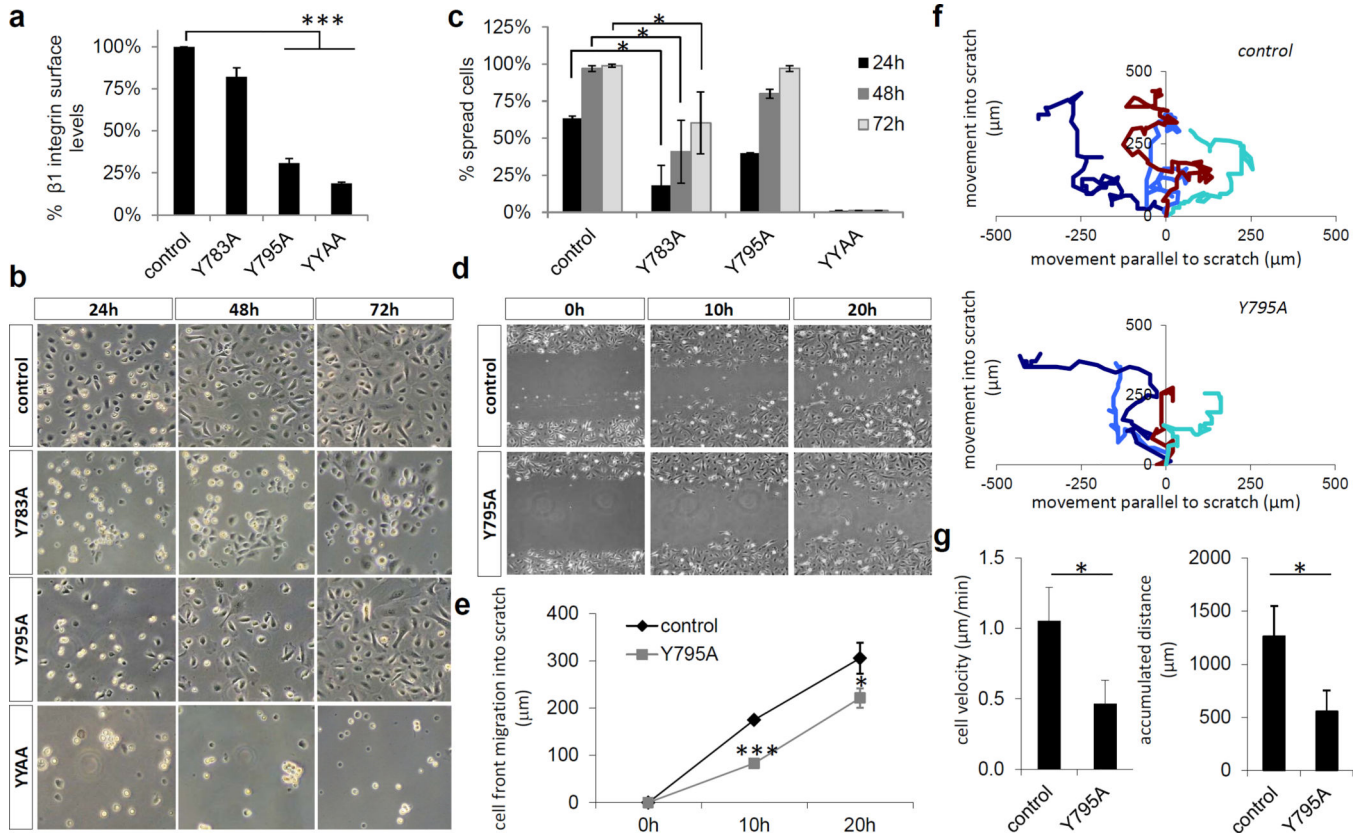


Figure 4. Adhesion and migration of $\beta 1$ Y-to-A keratinocytes

(a) Epidermis-derived single cell suspensions of normal and $\beta 1$ Y-to-A epidermis were assayed for $\beta 1$ integrin surface expression (mean \pm SD; n=4; *** P <0.0001 vs. control). (b) Adhesion of normal and $\beta 1$ Y-to-A keratinocytes to fibronectin and collagen coated tissue culture plastic over the indicated time period. (c) Spreading of normal and $\beta 1$ Y-to-A keratinocytes on fibronectin and collagen coated tissue culture plastic (mean \pm SD; n=3; * P <0.05 vs. control). (d) Scratch wounding of a confluent monolayer of normal and $\beta 1$ Y795A keratinocytes. (e) Quantification of cell front migration into a scratch wound (mean \pm SD; n=3; * P <0.05, *** P <0.0001 vs. control). (f) Assessment of migratory directionality. (g) Quantification of keratinocyte migratory velocity and accumulated distance (mean \pm SD; n=3; * P <0.05 vs. control).

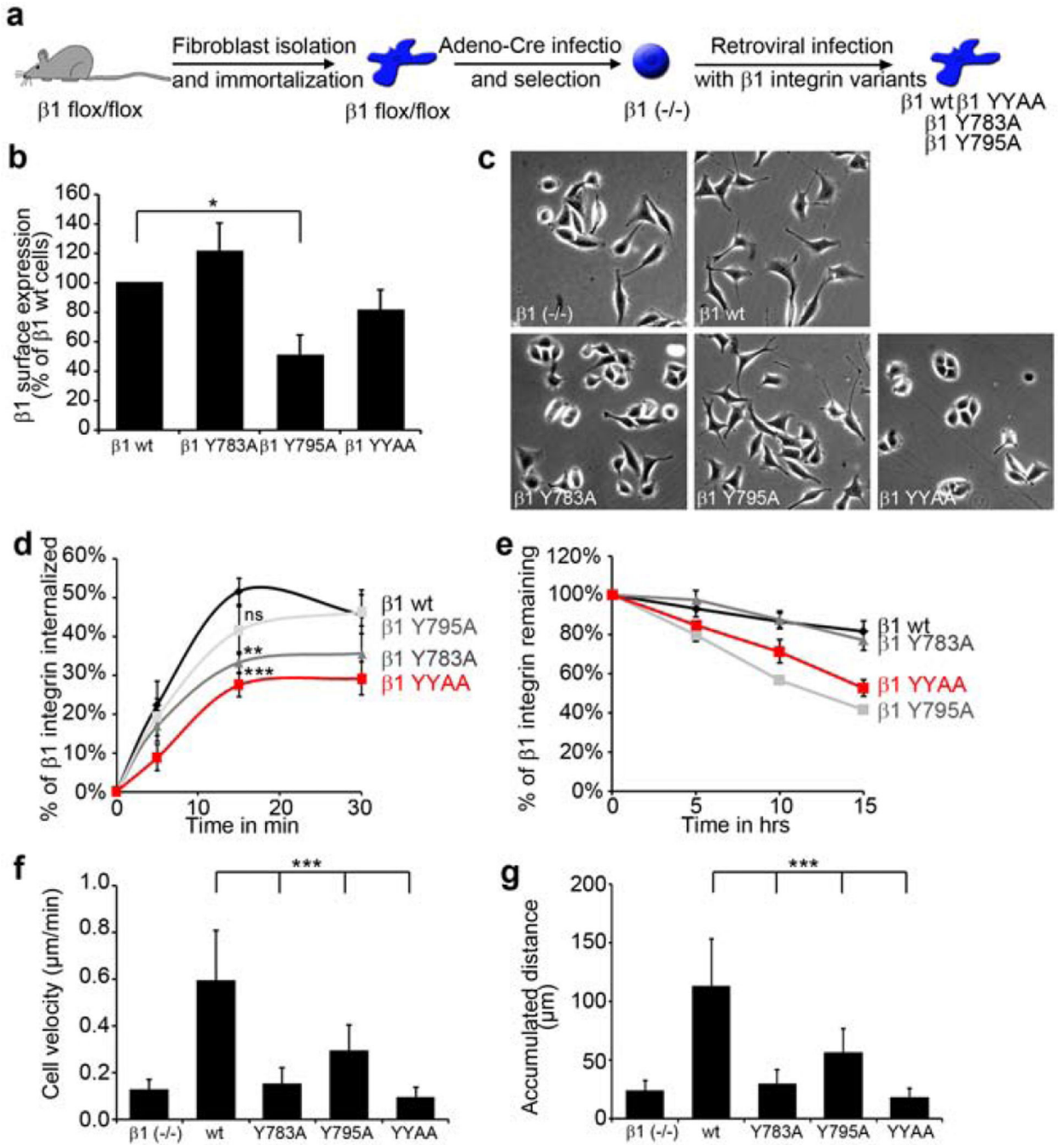


Figure 5. Effect of $\beta 1$ Y-to-A mutations on $\beta 1$ integrin stability, internalization and migration
(a) Scheme depicting the generation of wild-type (wt) and $\beta 1$ Y-to-A expressing fibroblasts.
(b) $\beta 1$ integrin surface levels as determined by FACS (mean \pm SD; n=3; * P <0.05). **(c)** Phase contrast images of $\beta 1$ integrin reconstituted fibroblasts. **(d)** Quantification of cell surface $\beta 1$ integrin internalization (mean \pm s.e.m.; n=5; ** P <0.005; *** P <0.001 vs. control). ns; not significant. **(e)** Quantification of cell surface $\beta 1$ integrin stability (mean \pm SD; n=3). **(f–g)** Quantification of fibroblast velocity **(f)** and accumulated distance **(g)** (mean \pm SD; n=30 cells from three movies; *** P <0.0001 vs. control).

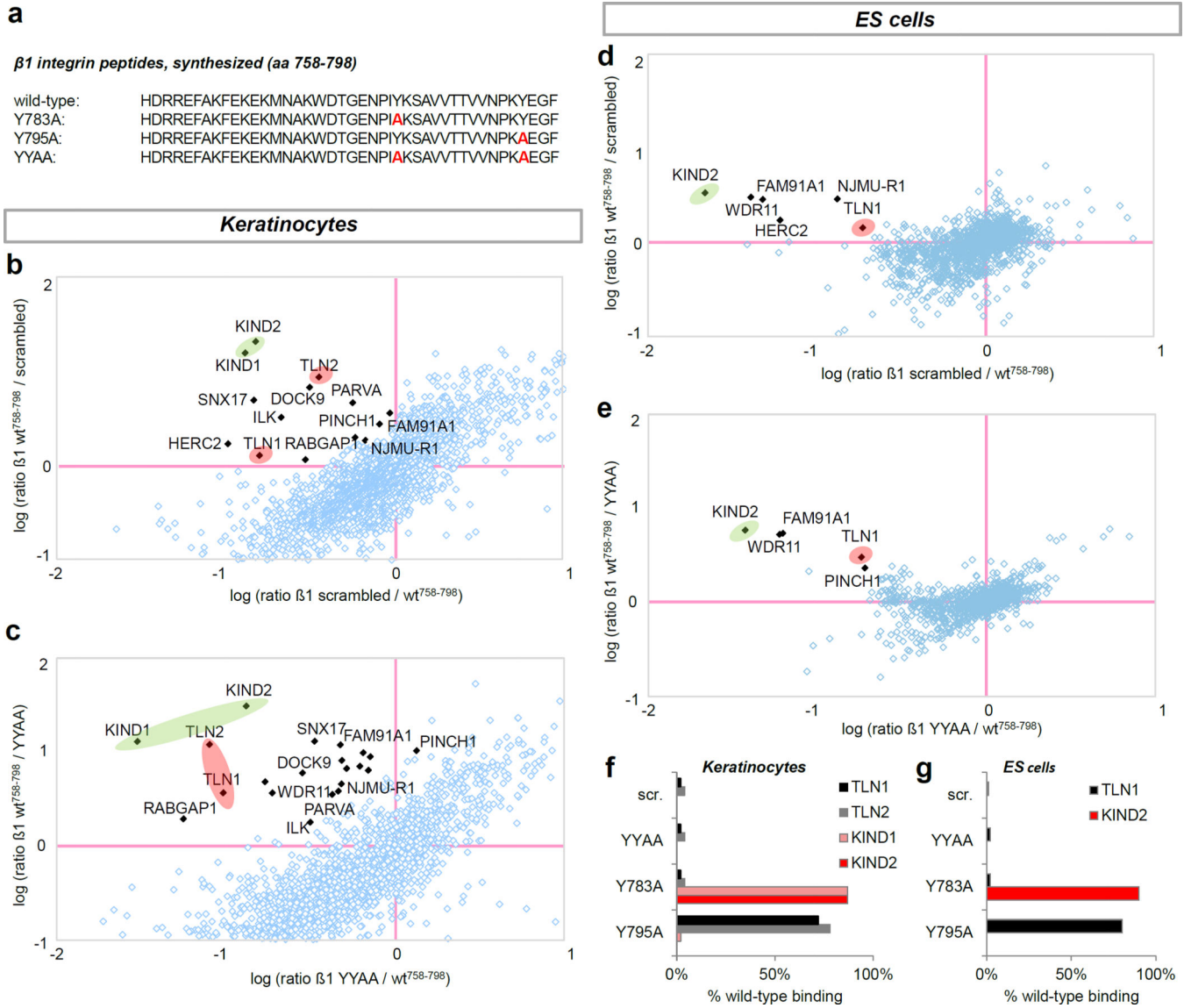


Figure 6. *β1* integrin cytoplasmic Y-to-A mutations impair protein recruitment in keratinocytes and ES cells

(a) Amino acid sequence of synthesized *β1* integrin peptides. (b–e) Loss in protein binding vs. wild-type peptide in keratinocytes using scrambled (b) and *β1* YYAA peptides (c). Loss in protein binding vs. wild-type peptide in ES cells using scrambled (d) and *β1* YYAA peptides (e). Scatter plots highlights kindlins (red circles) and talins (green circles). (f–g) Quantification of talin and kindlin binding to *β1* Y-to-A peptides relative to wild-type using keratinocyte (f) or ES cell lysates (g).